EXPERIMENTAL PERFORMANCE ANALYSIS OF AN ELECTROMAGNETIC ENERGY HARVESTER DRIVEN BY FLOW-INDUCED VIBRATION

Subekti[*], Paduloh[**], Mochamad Saidiman[***]

[*]*Department of Mechanical Engineering, Faculty of Industrial Engineering, Universitas Mercu Buana, Jakarta, Indonesia, subekti@mercubuana.ac.id*

[**]*Department of Industrial Engineering, Faculty of Engineering, Universitas Bhayangkara Jakarta Raya, Bekasi, Indonesia, paduloh@dsn.ubharajaya.ac.id*

[***]*Department of Industrial Engineering, Faculty of Creative Industrial, Universitas Teknologi Bandung, Bandung, Indonesia, m.saidiman@utb-univ.ac.id*

Email Correspondence: subekti@mercubuana.ac.id

Received : January 14, 2026 Accepted : May 24, 2026 Published : June 30, 2026

Abstract: This study aims to experimentally investigate the performance of an electromagnetic energy harvester driven by flow-induced vibration (FIV) under airflow conditions representative of building ventilation systems. A cylindrical oscillator integrated with a magnet–coil transduction mechanism was tested in a wind tunnel at airflow velocities of 0.5 m/s, 2 m/s, and 4 m/s. Vibration responses were measured using an FFT analyzer, while the electrical output was recorded using a digital oscilloscope and processed to obtain RMS voltage and average power. The results show that the harvested power at 2 m/s is approximately four times that obtained at 0.5 m/s, indicating optimal performance within the lock-in region, where the vortex-shedding frequency approaches the structure's natural frequency. Although higher airflow velocity increases the vibration amplitude, the average harvested power at 4 m/s decreases due to partial detuning and increased damping. These findings demonstrate that moderate airflow velocities provide optimal operating conditions for electromagnetic energy harvesting and highlight the feasibility of integrating airflow-based vibration energy harvesters into building systems to power low-energy devices.

Keywords: electromagnetic energy harvesting; flow-induced vibration; vortex-induced vibration; airflow velocity; structural vibration

Abstrak: Penelitian ini bertujuan untuk mengkaji secara eksperimental kinerja pemanen energi elektromagnetik yang digerakkan oleh getaran akibat aliran fluida (flow-induced vibration) pada kondisi aliran udara yang merepresentasikan sistem ventilasi bangunan. Sebuah silinder elastis yang terintegrasi dengan mekanisme transduksi magnet–kumparan diuji di dalam terowongan angin pada kecepatan aliran 0,5 m/s, 2 m/s, dan 4 m/s. Respons getaran diukur menggunakan FFT analyzer, sedangkan keluaran listrik direkam menggunakan osiloskop digital dan dianalisis untuk memperoleh tegangan RMS serta daya rata-rata. Hasil penelitian menunjukkan bahwa daya yang dihasilkan pada kecepatan 2 m/s sekitar empat kali lebih besar dibandingkan dengan 0,5 m/s, yang menunjukkan kondisi operasi optimal pada daerah lock-in ketika frekuensi pelepasan pusaran mendekati frekuensi alami struktur. Meskipun peningkatan kecepatan aliran memperbesar amplitudo getaran, daya rata-rata pada 4 m/s menurun akibat efek detuning

parsial dan peningkatan redaman sistem. Temuan ini menunjukkan bahwa kecepatan aliran sedang merupakan kondisi optimal untuk pemanenan energi elektromagnetik serta menegaskan potensi integrasi sistem ini pada infrastruktur bangunan untuk menyuplai perangkat berdaya rendah.

Kata kunci: Pemanenan energi elektromagnetik; getaran akibat aliran; vortex-induced vibration; kecepatan aliran; getaran struktur

Recommended APA Citation :

Subekti, Paduloh, & Saidiman, M. (2026). Experimental Performance Analysis of an Electromagnetic Energy Harvester Driven by Flow-Induced Vibration. *Elkawnie*, *12*(1), 29-46. https://doi.org/10.22373/ekw.v12i1.33750

Introduction

Energy is a fundamental driver of human civilization and technological advancement. With the continuous increase in global energy demand and the urgent need to reduce reliance on fossil fuels, energy harvesting has emerged as a promising approach for converting ambient energy into usable electrical power at a local scale. In urban environments, airflow generated in high-rise buildings—particularly within heating, ventilation, and air-conditioning (HVAC) ducting systems—is continuously available due to pressure differences and mechanical ventilation. This persistent airflow represents an underutilized source of kinetic energy suitable for small-scale energy harvesting applications. The urban building environment and HVAC ducting airflow constitute the object of this study (Figure. 1), while the research focuses on harvesting this airflow-induced kinetic energy through flow–structure interaction mechanisms.



Figure 1. Airflow availability in high-rise buildings and HVAC ducting systems as a potential kinetic energy source.

Despite the continuous availability of airflow in HVAC ducting systems, converting this dispersed and low-density kinetic energy into stable and usable electrical output remains a significant challenge. One widely investigated

mechanism for inducing strong and repeatable mechanical excitation is flow-induced vibration (FIV), particularly vortex-induced vibration (VIV). VIV occurs when fluid flows past a bluff body, such as a circular cylinder, resulting in periodic vortex shedding that generates alternating lift forces transverse to the flow direction. These forces induce structural oscillations, especially when the Reynolds number exceeds the critical threshold for vortex instability. This oscillatory behavior provides a reliable mechanical energy source that can be converted into electrical power. The fundamental mechanism of VIV and transverse oscillations generated from a cylindrical oscillator is shown in Figure. 2.

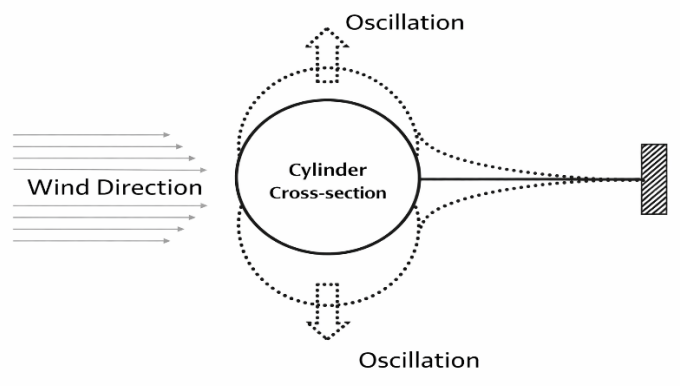


Figure 2. Schematic of vortex-induced vibration of a circular cylinder under airflow.

Recent studies have demonstrated the feasibility of harvesting energy from flow-induced and vortex-induced vibrations under a wide range of flow conditions. However, despite substantial progress, most existing works remain limited in three key aspects. First, many studies are conducted under idealized or steady flow conditions, which do not fully represent the fluctuating and constrained airflow characteristics inside HVAC ducting systems. Second, while synchronization (lock-in) behavior is known to be critical for maximizing energy output, its dependence on electromechanical coupling and electrical loading conditions is still not fully understood, particularly for electromagnetic transduction systems. Third, although both piezoelectric and electromagnetic harvesters have been widely investigated, comparative insights into their performance trade-offs in realistic building airflow environments remain insufficient.

Comprehensive reviews published in the last five years highlight that FIV- and VIV-based energy harvesters are particularly suitable for low-power applications such as wireless sensors and Internet-of-Things (IoT) devices due to their scalability and robustness (Wang et al., 2022; Zhang et al., 2024). Experimental and numerical studies have shown that vibration amplitude, synchronization range (lock-in), and harvested power strongly depend on bluff-body geometry, Reynolds number, and electromechanical coupling strategy (Dai et al., 2024; Kumar et al., 2022). Furthermore, recent advances indicate that

electromagnetic and nonlinear coupling mechanisms can significantly enhance bandwidth and power output compared to conventional linear systems, especially under variable airflow conditions (Li et al., 2022).

The current state of the art in flow-induced vibration energy harvesting emphasizes compact, lightweight, and highly efficient systems capable of operating under realistic and variable flow conditions. Recent research trends focus on optimizing bluff-body geometry, expanding the synchronization range, and integrating electromagnetic or hybrid transduction mechanisms to improve power density and adaptability (Zhao et al., 2021). However, despite these advancements, there remains a lack of systematic investigation on electromagnetic VIV harvesters specifically designed for HVAC duct environments, particularly with respect to the coupled effects of Reynolds number variation, lift-induced oscillation behavior, and electrical load (R–L) matching for optimal power extraction.

In line with these research gaps, the present study proposes an electromagnetic energy harvester based on a cylindrical oscillator exposed to airflow within HVAC ducting systems (Figure. 1), operating under the VIV mechanism illustrated in Figure. 2. Unlike previous studies, which have largely focused on piezoelectric energy harvesting (pzEH) in HVAC duct systems (Gkoumas et al., 2017; Weinstein et al., 2012), piezoelectric approaches are limited by material cost, durability constraints, and dependence on intrinsic coupling coefficients. This research instead targets airflow-based electromagnetic energy harvesting in building infrastructure, with a specific emphasis on optimizing Reynolds number, lift-induced oscillations, and electrical load (R–L) parameters to maximize harvested power. By addressing these gaps, the proposed system provides a more practical and scalable solution for sustainable energy harvesting integrated into building environments.

Methods

Flow-Induced Vibration Analysis

The flow regime around the circular cylinder is characterized using the Reynolds number:

$$Re = \frac{\rho U D}{\mu} \quad \text{..... (1)}$$

This formulation is standard in fluid mechanics and remains valid across contemporary studies (White, 2011). The Reynolds number is used to ensure that the flow condition lies within the vortex-shedding regime, which has been confirmed experimentally in recent FIV/VIV energy harvesting investigations (Dai et al., 2024).

When airflow passes the cylinder, alternating vortices are shed, generating a periodic lift force that induces transverse oscillations. As the vortex shedding frequency approaches the natural frequency of the system, synchronization (*lock-*

in) occurs, resulting in maximum vibration amplitudes within a bounded range. This phenomenon has been extensively observed in recent experimental and numerical studies on airflow-induced vibration energy harvesting. (Hu, et al., 2020).

Mechanical–Electromagnetic Coupling

The dynamic behavior of the system is modeled as a mass–spring–damper system subjected to lift excitation:

$$m\ddot{y}(t) + c\dot{y}(t) + ky(t) = F_L(t) \text{ .... (2)}$$

This formulation remains the standard approach for modeling vibration-based energy harvesters and continues to be used in recent electromagnetic harvesting studies. (Indah, et al., 2023).
The lift force acting on the cylinder is expressed as:

$$F_L(t) = \frac{1}{2}\rho U^2 DLC_L(t) \text{ .... (3)}$$

where the lift coefficient variation is modeled as a harmonic function, consistent with recent VIV-based harvesting models (Zhu, eet al., 2023).

Electromagnetic Energy Conversion

The electromagnetic energy harvesting mechanism follows Faraday's law of electromagnetic induction, whereby relative motion between a magnet and a coil induces an electromotive force:

$$V(t) = NBl\dot{y}(t) \text{ .... (4)}$$

Although Faraday's law is classical, its application to micro- and mesoscale vibration energy harvesting systems remains central to recent electromagnetic harvester designs (Li et al., 2022; Indah et al., 2023). The instantaneous electrical power delivered to the load resistance R_L is given by:

$$P(t) = \frac{V^2(t)}{R_L} \text{ ....(5)}$$

Materials

The experimental setup consists of an electromagnetic vibration energy harvesting system driven by flow-induced vibrations (FIV). The system employs an elastically supported circular cylinder exposed to uniform airflow, a configuration that has been widely adopted in recent studies on airflow-based energy harvesting applications, particularly in building and HVAC environments. (Roundy, et al., 2003; (Chung et al., 2023).

The test cylinder is fabricated from polycarbonate with an outer diameter of $D = 0.045$ m, length $L = 0.32$ m, and mass $m = 0.06642$ kg. The elastic support consists of a stainless-steel beam (Young's modulus 206 GPa), enabling cross-flow oscillations induced by lift forces. Similar elastically supported bluff-body

configurations have been recently employed for vortex-induced vibration energy harvesting systems. (Djanali, 2024; Subekti, et al., 2022)

The electromagnetic energy harvesting subsystem comprises a permanent magnet attached to the vibrating structure and a stationary coil positioned to capture relative motion. This electromagnetic transduction approach is increasingly favored in recent vibration energy harvesting studies due to its lightweight design and robustness under variable excitation conditions. (Hammid & Surjosatyoe, 2018).

Airflow is supplied using a wind tunnel with controlled wind velocities of 0.5 m/s, 2 m/s, and 4 m/s. Vibration measurements are obtained using an FFT analyzer, while voltage signals are recorded using a digital oscilloscope and processed using MATLAB. Comparable experimental arrangements have been reported in recent airflow-based and structural vibration energy harvesting research. (Mashuri, et al., 2024; Subekti, et al., 2024; Syahputra, et al., 2024; Andriansyah, et al., 2024; Suryadi, et al., 2024).

Instrumentation

The experimental investigation employed several measurement and data acquisition instruments to characterize the vibration response and electrical output of the electromagnetic energy harvesting system. Airflow velocity was controlled and monitored using a laboratory-scale wind tunnel equipped with a digital anemometer (model: BENETECH GM816, Benetech Instruments, China). Structural vibrations of the elastically supported cylinder were measured using an FFT Analyzer (model: ONO SOKKI CF-9400, Ono Sokki Co., Ltd., Japan), which enabled time-domain and frequency-domain analysis of vibration signals.

The electrical output generated by the electromagnetic energy harvester was measured using a digital oscilloscope (model: Hantek 6022BE, Hantek Electronic Co., Ltd., China). The oscilloscope was connected to a personal computer via USB interface, allowing voltage signals to be recorded and analyzed in real time. Signal processing and post-analysis were performed using MATLAB software (R2023a, MathWorks Inc., USA). Similar instrumentation configurations have been widely adopted in recent vibration-based energy harvesting studies (Lian et al., 2017; Shaker et al., 2026; Dubey et al., 2026; Tang et al., 2026). The conceptual framework of the proposed airflow-based energy harvesting system is shown in Figure. 3.

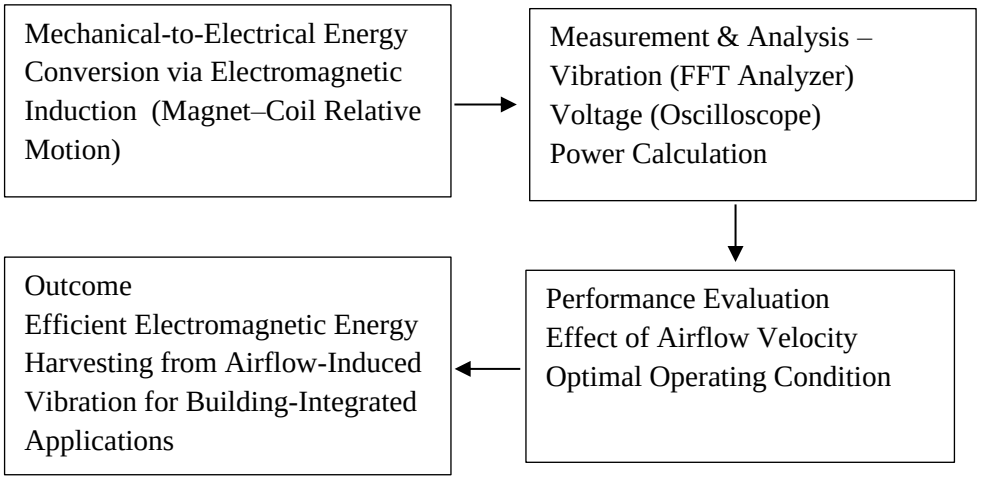


Figure 3. Conceptual framework of the proposed airflow-based energy harvesting system.

The experimental procedure followed established methodologies for flow-induced vibration and electromagnetic energy harvesting experiments. The elastically supported circular cylinder was mounted inside the wind tunnel test section with its axis perpendicular to the airflow direction. Airflow velocity was gradually adjusted and stabilized at 0.5 m/s, 2 m/s, and 4 m/s. At each airflow velocity, vibration signals were recorded under steady-state conditions using an FFT analyzer. The measured time-domain signals were then transformed into the frequency domain using Fast Fourier Transform (FFT) techniques. Simultaneously, the voltage generated by the electromagnetic harvester was measured across a fixed load resistance using a digital oscilloscope. The recorded voltage signals were processed in MATLAB to obtain RMS voltage values and corresponding electrical power outputs. This procedure was repeated for all airflow conditions to enable comparative performance evaluation.

.

Results and Discussion

This section presents the experimental results and their corresponding analyses to evaluate the performance of the electromagnetic energy harvesting system driven by airflow-induced vibration. The discussion begins with the identification of the flow regime using the Reynolds number to confirm the occurrence of vortex shedding. Subsequently, the vibration characteristics, frequency response, electrical voltage generation, and harvested power are analyzed and correlated with airflow velocity. The experimental observations are interpreted using relevant theoretical relations to explain the underlying physical mechanisms governing the energy harvesting performance.

Flow Regime Identification Using Reynolds Number

To confirm that the cylinder operates in the vortex-shedding regime, the Reynolds number is calculated for each airflow velocity using Equation 1, where the

parameters used are ρ=1.225 kg/m3, μ=1.81×10−5 Pa·s, and D = 0.045m. So that the value of the Reynolds number produced due to the given wind speed will be obtained as shown in Table 1.

Table 1. The Reynolds number produced due to the given wind speed

Airflow Velocity	Numerator	Reynolds Number
U = 0.5 m/s	$\rho UD = 1.225 \times 0.5 \times 0.045 = 0.0275625$	$Re = \frac{0.0275625}{1.81 \times 10^{-5}} \approx 1523$
U = 2 m/s	$\rho UD = 1.225 \times 2 \times 0.045 = 0.11025$	$Re = \frac{0.11025}{1.81 \times 10^{-5}} \approx 6097$
U = 4 m/s	$\rho UD = 1.225 \times 4 \times 0.045 = 0.2205$	$Re = \frac{0.2205}{1.81 \times 10^{-5}} \approx 12182$

All calculated Reynolds numbers are well above the onset of vortex shedding for circular cylinders (commonly cited around. $Re > 40$), confirming that the experiments are conducted in the VIV-capable regime. This supports the vibration observations in Figure 6–Figure 7, where oscillation amplitude and modal richness increase with airflow velocity.

Estimating Vortex Shedding Frequency Using Strouhal Number

The vortex shedding frequency can be estimated using the Strouhal relationship (Chassaing, 2023).

$$f = St\frac{U}{D} \quad \text{..... (6)}$$

Assuming $St = 0.20$ and $D = 0.045$ mUsing equation (6), the vortex shedding frequency will be obtained as shown in Table 2.

Table 2. The vortex shedding frequency

Airflow Velocity	Vortex Shedding Frequency
U = 0.5 m/s	$f_s = 0.20\frac{0.5}{0.045} = 0.20 \times 11.111 \approx 2.22$ Hz
U = 2 m/s	$f_s = 0.20\frac{2}{0.045} = 0.20 \times 44.444 \approx 8.89$ Hz
U = 4 m/s	$f_s = 0.20\frac{4}{0.045} = 0.20 \times 88.889 \approx 17.78$ Hz

FFT vibration analysis indicates that the dominant structural vibration frequency is approximately 16 Hz. The estimated vortex shedding frequencies suggest that synchronization may occur depending on the interaction between flow velocity, mass ratio, and system damping. Therefore, experimental observations presented in Figures 7 and 10–12 are essential for identifying the optimal operating

condition, as maximum harvested power may occur within the lock-in region even when the estimated shedding frequency does not perfectly match the natural frequency.

Linking Airflow Velocity to Lift Force Scaling

The time-domain vibration amplitude increase in Figure 6 can be explained through the lift force magnitude, which scales with U^2:

$$F_L(t) = \frac{1}{2}\rho U^2 DL\, C_L(t) \qquad (7)$$

Table 3 shows the dynamic pressure ($q = \frac{1}{2}\rho U^2$) generated due to airflow velocity.

Table 3. Dynamic pressure due to changes in airflow velocity

Airflow Velocity	Dynamic Pressure
U = 0.5 m/s	$q = \frac{1}{2}(1.225)(0.5^2) = 0.153$ Pa
U = 2 m/s	$q = \frac{1}{2}(1.225)(2^2) = 2.45$ Pa
U = 4 m/s	$q = \frac{1}{2}(1.225)(4^2) = 9.8$ Pa

From 0.5 to 2 m/s, $q$increases from 0.153 to 2.45 Pa (≈ **16×**), and from 2 to 4 m/s, it increases further to 9.8 Pa (≈ **4×**). This explains why vibration amplitude tends to rise strongly with airflow velocity, consistent with the time-domain results.

Electromagnetic Voltage Calculation from Measured Vibration Velocity

The induced voltage follows Faraday-type proportionality to relative velocity:

$$v(t) = K_e \dot{y}(t) \qquad (8)$$

where $K_e$is an effective electromechanical constant (lumping N, B, coil geometry, and coupling).

How to compute from your oscilloscope data (Figure 8):

1. Export the sampled voltage signal $v(t)$.
2. Compute RMS voltage:

$$V_{\text{rms}} = \sqrt{\frac{1}{T}\int_0^T v^2\,(t)\,dt} \qquad (9)$$

(Optional) If the waveform is close to sinusoidal with peak voltage (V_p) (Boylestad, & Nashelsky, 2011):

$$V_{\text{rms}} \approx \frac{V_p}{\sqrt{2}} \qquad (10)$$

This is why voltage amplitude may not scale linearly with displacement amplitude: voltage depends on velocity and coupling, and can be reduced by increased damping or detuning effects even when displacement looks larger.

Power Calculation

The instantaneous electrical power delivered to a resistive load is:

$$p(t) = \frac{v^2(t)}{R_L} \quad \text{(11)}$$

The average power over a window *T* is:

$$P_{\text{avg}} = \frac{1}{T}\int_0^T \frac{v^2(t)}{R_L}\, dt = \frac{V_{\text{rms}}^2}{R_L} \quad \text{(12)}$$

For each airflow velocity (0.5, 2, 4 m/s), report:

- R_L =(your value)
- V_{rms} =(computed from oscilloscope data)
- $P_{\text{avg}} = V_{\text{rms}}^2/R_L$

finding ("4× at 2 m/s"). Once the three P_{avg}values are computed, you can state the ratio explicitly:

$$\frac{P_{\text{avg, 2}}}{P_{\text{avg, 0.5}}} \approx 4 \quad \text{(13)}$$

and then interpret why 2 m/s produces higher average power than 4 m/s using the lock-in/detuning argument supported by the frequency plots (Figure 6 and Figure 8) and by the fact that higher excitation can increase damping losses and reduce synchronization.

Experimental Setup and Flow Conditions

The experimental configuration used to investigate the vibration response and energy harvesting performance is presented in Figure 4. The elastically supported circular cylinder integrated with the electromagnetic vibration energy harvester was placed inside the wind tunnel test section. The airflow was directed perpendicular to the cylinder axis to promote cross-flow excitation dominated by lift forces. Airflow velocity was varied at three discrete values, namely 0.5 m/s, 2 m/s, and 4 m/s, representing low to moderate flow conditions commonly encountered in building ducting systems.

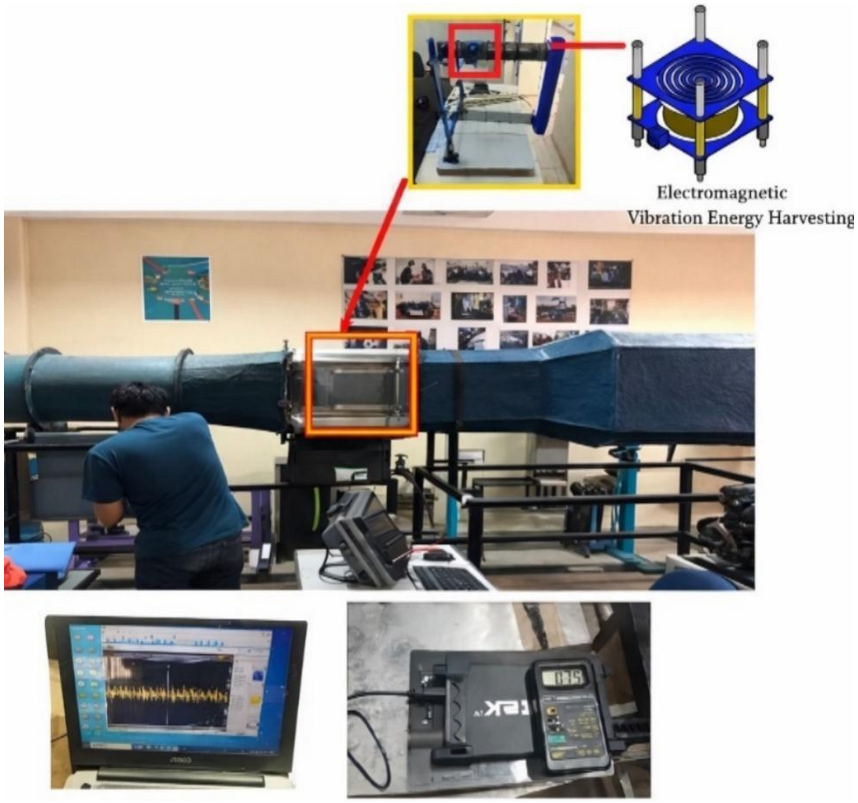


Figure 4. Experimental setup of the elastically supported cylinder with electromagnetic vibration energy harvester inside the wind tunnel (Subekti et al., 2025; Wu et al., 2026).

This configuration ensures that vortex shedding occurs in the wake of the cylinder and induces transverse oscillations, which are essential for vortex-induced vibration (VIV)-based energy harvesting.

Time-Domain Vibration Response

The time-domain vibration responses of the elastically supported cylinder measured using the FFT analyzer are shown in Figure 5. The results indicate that vibration amplitude increases with increasing airflow velocity. At a low airflow velocity of 0.5 m/s, the oscillation amplitude is relatively small, indicating weak vortex shedding and limited excitation energy. As the airflow velocity increases to 2 m/s and 4 m/s, the vibration amplitude increases significantly due to stronger vortex-induced lift forces acting on the cylinder.

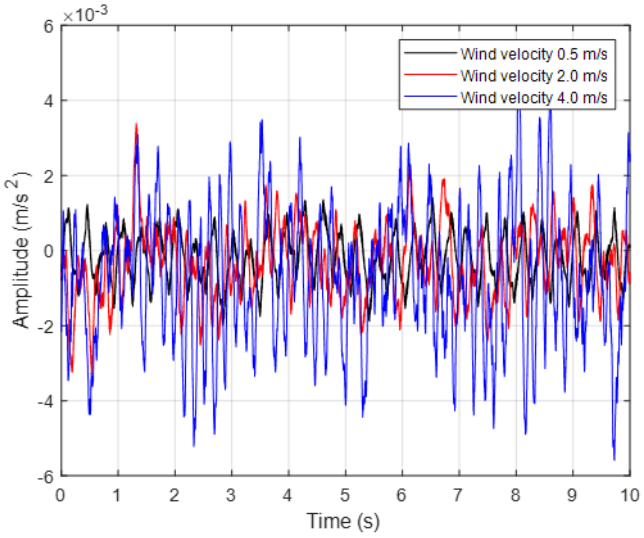


Figure 5. Time-domain vibration response of the elastically supported cylinder at different airflow velocities.

This behavior confirms that the vibration response is strongly dependent on airflow velocity and that the system operates within the vortex-induced vibration regime. The increasing amplitude reflects enhanced energy transfer from the fluid to the structure as the Reynolds number increases.

Frequency-Domain Vibration Analysis

Further analysis of the vibration response was conducted using Fast Fourier Transform (FFT), and the corresponding frequency-domain results are presented in Figure 6. The dominant vibration frequency is observed to remain approximately constant at around 16 Hz for all airflow velocities. This indicates that the vibration response is governed primarily by the natural frequency of the elastically supported system.

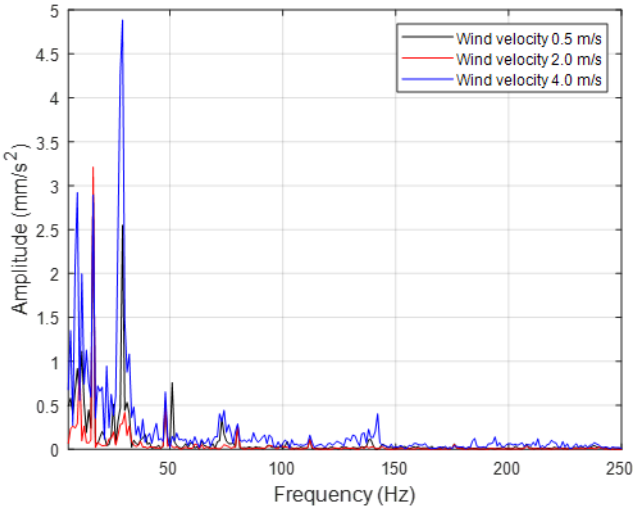


Figure 6. Frequency-domain (FFT) vibration response of the elastically supported cylinder.

Although the dominant frequency remains unchanged, the number of excited vibration modes increases with airflow velocity. At an airflow velocity of 2 m/s, six dominant vibration modes are observed, whereas at 4 m/s, the number increases to eleven modes. This increase in modal content is attributed to higher Reynolds numbers, which intensify vortex shedding and excite additional dynamic responses in the structure. These results demonstrate that increasing airflow velocity enhances the complexity of the vibration response rather than shifting the dominant frequency.

Time-Domain Voltage Response

The voltage output generated by the electromagnetic energy harvester was measured using a digital oscilloscope, and the time-domain voltage signals are presented in Figure 7. The measured voltage amplitudes are relatively small, on the order of millivolts, and do not show a significant increase with airflow velocity.

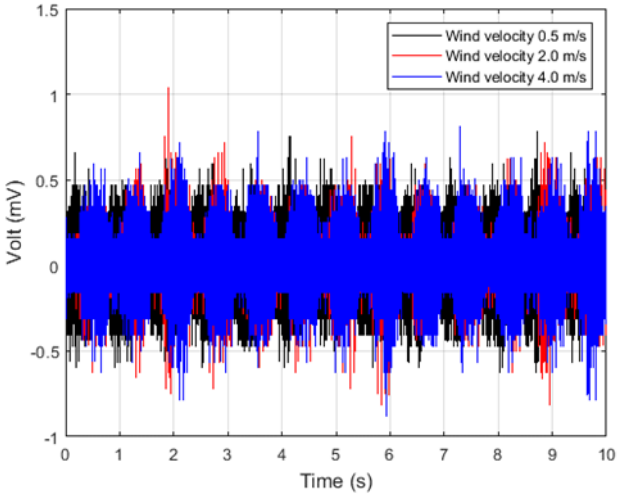


Figure 7. Time-domain voltage output of the electromagnetic energy harvester at different airflow velocities.

This observation suggests that voltage amplitude alone does not directly represent the harvesting performance. Although higher airflow velocities produce larger mechanical vibrations, the electromagnetic coupling efficiency and system damping also play important roles in determining the electrical output.

Frequency-Domain Voltage Analysis

To further investigate the electrical response, FFT analysis was applied to the voltage signals, and the frequency-domain results are shown in Figure 8. At an airflow velocity of 0.5 m/s, the voltage spectrum exhibits a distinct dominant frequency, indicating stable synchronization between mechanical vibration and electromagnetic induction.

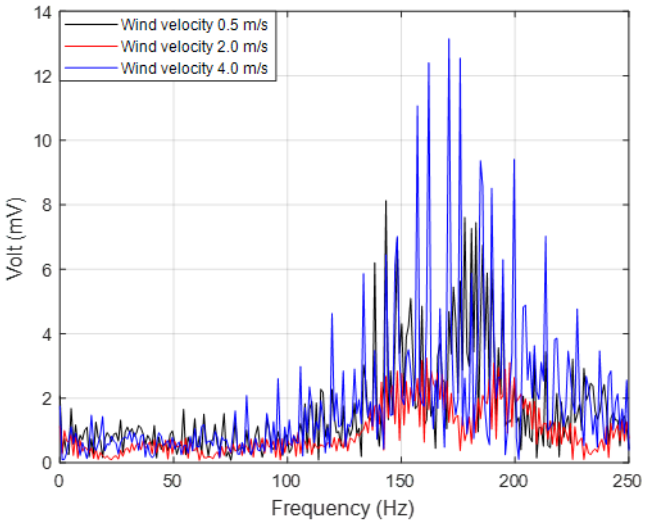


Figure 8. Frequency-domain (FFT) voltage response of the electromagnetic energy harvester.

At higher airflow velocities of 2 m/s and 4 m/s, the voltage spectrum becomes more distributed, with multiple frequency components appearing. This behavior suggests that the system partially departs from the optimal lock-in condition, resulting in reduced synchronization efficiency between mechanical motion and electrical energy conversion. These results highlight the importance of operating within the synchronization range to achieve efficient energy harvesting.

Power Output at Different Airflow Velocities

The electrical power output was calculated based on the measured voltage and load resistance. The power generated at an airflow velocity of 0.5 m/s is shown in Figure 9. At this velocity, the harvested power is relatively low, indicating insufficient excitation energy to drive effective electromagnetic conversion.

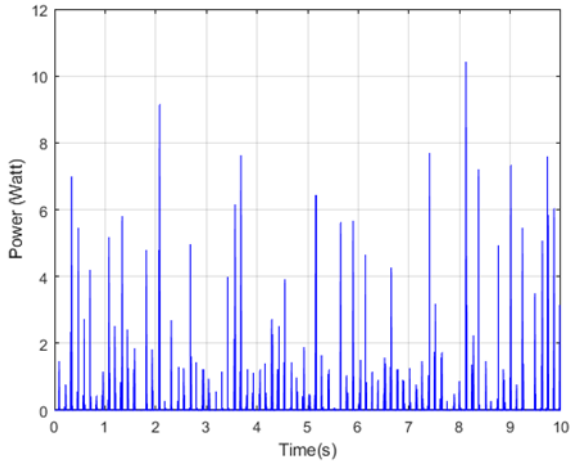


Figure 9. Electrical power output at an airflow velocity of 0.5 m/s.

When the airflow velocity increases to 2 m/s, the harvested power increases by approximately four times compared to the 0.5 m/s condition, as shown in Figure 10. This significant improvement indicates that the system reaches an optimal operating condition at this velocity, where vortex shedding frequency closely matches the natural frequency of the structure.

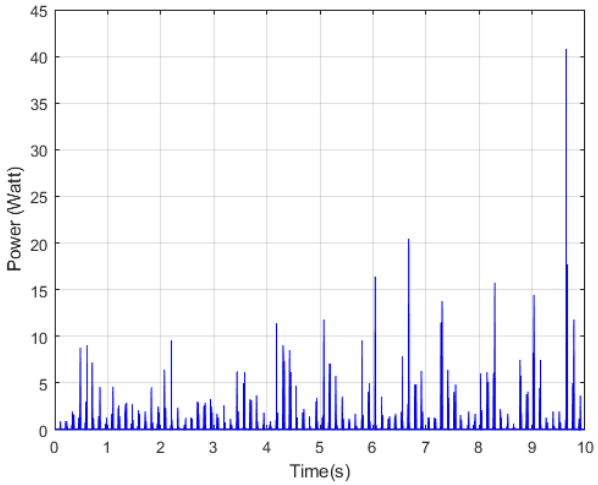


Figure 10. Electrical power output at an airflow velocity of 2 m/s.

At an airflow velocity of 4 m/s, the power output is shown in Figure 11. Although the instantaneous peak power is higher than that observed at 2 m/s, the average power output is lower. This reduction is attributed to increased damping and reduced elastic efficiency of the spring–mass system at higher excitation levels, causing the system to operate partially outside the lock-in region.

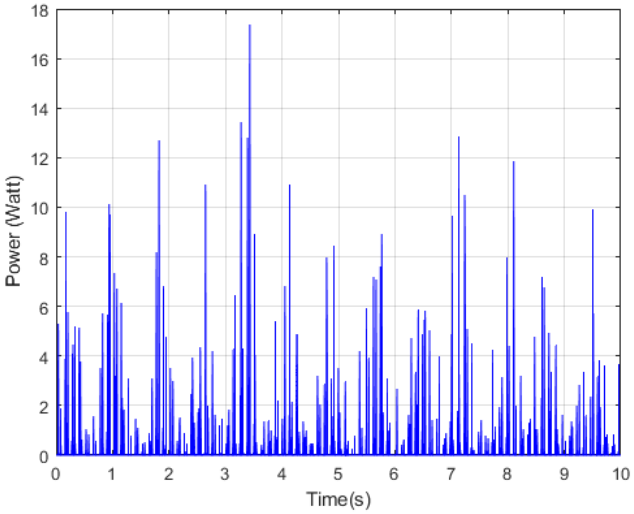


Figure 11. Electrical power output at an airflow velocity of 4 m/s.

Discussion and Engineering Implications

The experimental results demonstrate that electromagnetic energy harvesting from airflow-induced vibrations is highly sensitive to the interaction between airflow velocity, structural dynamics, and electromagnetic coupling. The optimal performance observed at an airflow velocity of 2 m/s highlights the critical role of the lock-in phenomenon in maximizing average harvested power (Jiang et al., 2022). These findings are particularly relevant for airflow energy harvesting applications in building ducting systems, where airflow velocities typically fall within the low-to-moderate range. The results confirm that increasing airflow velocity does not necessarily lead to higher average power output, emphasizing the importance of resonance tuning and system optimization.

Overall, the study validates the feasibility of harvesting electrical energy from vortex-induced vibrations using an electromagnetic transduction mechanism and provides experimental insights for designing efficient airflow-based energy harvesting systems for building-integrated applications.

Conclusion

This study examines electromagnetic energy harvesting from airflow-induced vibrations of a circular cylinder undergoing vortex-induced vibration. Results show that airflow velocity strongly affects vibration behavior, electrical output, and harvested power. Higher velocities increase vibration amplitude and trigger additional modes, but the dominant frequency remains tied to the structure's natural frequency. Efficient energy conversion depends on synchronization between mechanical motion and electromagnetic response, not just voltage magnitude. Maximum average power occurs at 2 m/s within the lock-in region, where vortex shedding and natural frequencies align. At higher velocities, performance declines due to damping and loss of synchronization. Overall, the study demonstrates the feasibility of this method for building applications and highlights its potential to power low-energy devices in smart building systems.

Conflict of Interest

The authors declare no conflict of interest. All authors contributed to the research and manuscript preparation. Artificial Intelligence tools were used only for language editing and formatting assistance and did not influence the scientific content or conclusions.

References

Andriansyah, F., Indah, N., & Subekti, S. (2024). Harvesting energy vibration derived from the rotational speed of a 4-stroke engine. *JTTM: Jurnal Terapan Teknik Mesin*, *5*(1), 67-74.

Boylestad, R. L., & Nashelsky, L. (2011). Electronic devices and circuit theory. *Pearson*.

Chassaing, P. (2023). Fundamentals of fluid mechanics. *Springer: Berlin/Heidelberg*,

Germany.

Chung, M. H., Yoo, S., Jung, W. N., Jeong, H., & Yoo, K. H. (2023). Self-powered airflow sensor based on energy harvesting of ventilation air in buildings. *Advanced Fiber Materials*, *5*(5), 1788-1798.

Dai, H., Abdelkefi, A., & Wang, L. (2024). Nonlinear dynamics and synchronization enhancement in vortex-induced vibration energy harvesters. *Nonlinear Dynamics*, *111*, 13455–13472. https://doi.org/10.1007/s11071-023-09187-6

Djanali, V. S. (2024). Identification of a nonlinear system for an elastically supported cylinder on cross-flow using wavelet transform. *Jordan Journal of Mechanical and Industrial Engineering*, *18*(1), 89–97. https://doi.org/10.59038/jjmie/180107

Dubey, D. K. (2026). Design and Optimization of Forced Transducers for Energy Harvesting from Ambient Mechanical Vibrations, Wind, and Ocean Waves. *Journal of Alternative and Renewable Energy Sources*, *12*(1), 1-10.

Gkoumas, K., Petrini, F., & Bontempi, F. (2017). Piezoelectric vibration energy harvesting from airflow in HVAC (heating, ventilation, and air conditioning) systems. *Procedia engineering*, *199*, 3444-3449.

Hammid, A., & Surjosatyoe, A. (2018). *The Use of Flow-Induced Vibration as An Alternative Source of New Power Plant in Indonesia*. *01017*, 1–6.

Hu, G., Tse, K. T., Wei, M., & Kwok, K. C. S. (2020). Experimental investigation of flow-induced vibration energy harvesting at low wind speeds. *Experimental Investigation of Flow-Induced Vibration Energy Harvesting at Low Wind Speeds*, *211*, 112726. https://doi.org/10.1016/j.enconman.2020.112726

Indah, N., Yunas, J., Hamzah, A. A., Latif, R., Sudrajat, N., Hamidah, I. (2023). NoStructural performance of PDMS-based planar membrane for electromagnetic vibration energy harvester. *International Journal of Nanoelectronics and Materials*, *16*, 385–393. https://doi.org/10.58915/ijneam.v16iDECEMBER.419

Jiang, W., Li, Y., Ma, X., Wang, Y., Chen, L., & Bi, Q. (2022). Exploiting internal resonance to improve flow energy harvesting from vortex-induced vibrations. *Journal of Intelligent Material Systems and Structures*, *33*(3), 459-473.

Kumar, R., Mishra, S., & Yadav, A. (2022). Effect of bluff body geometry on vortex-induced vibration energy harvesting. *Journal of Fluids and Structures*, *108*(10341). https://doi.org/10.1016/j.jfluidstructs.2021.103471

Kurniawan, I., Ichwani, R., Fionasari, R., Batubara, A., & Huda, A. (2022). Indonesia's renewable energy outlook: what to expect in the future renewable energy of Indonesia. a brief review. *Elkawnie: Journal of Islamic Science and Technology*, *8*(2), 298-313.

Li, S., Tang, L., Yang, Y., & Dowell, E. H. (2022). Broadband electromagnetic energy harvesting from vortex-induced vibration using nonlinear coupling. *Mechanical Systems and Signal Processing*, *168*, 108642. https://doi.org/10.1016/j.ymssp.2021.108642

Lian, J., Yan, X., Liu, F., & Zhang, J. (2017). *Analysis on Flow Induced Motion of Cylinders with Different* Cross *Sections and the Potential Capacity of Energy Transference from the Flow*. *2017*. https://doi.org/10.1155/2017/4356367

Mashuri, U. R., Hidayat, M. N., Efendy, B. D., & Subekti, S. (2024). FFT-based analysis of throttle body misfiring vibration. *JTTM*, *5*(2), 230–237. https://doi.org/10.37373/jttm.v5i2.1107

Roundy, S., Wright, P. K., & Rabaey, J. (2003). *A study of low level vibrations as a power source for wireless sensor nodes*. *26*, 1131–1144.

Shaker, M. R., Eluri, P. R., Ayele, F., & Chang, B. (2026). Practice and Feasibility of Energy Harvesting Technologies in Civil Infrastructure: A Comparative Review. *Sustainability*, *18*(4), 2055.

Subekti, S., Guntur, H. L., Djanali, V. S., & Syaifudin, A. (2024, October). Experimental identification an elastically supported cylinder under free vibration using the Hilbert and wavelet transform. In *AIP Conference Proceedings* (Vol. 3098, No. 1, p. 020037). AIP Publishing LLC.

Subekti, S., Guntur, H. L., Djanali, V. S., & Syaifudin, A. (2022). Simulation and dynamic system modeling of an elastically supported rigid cylinder for vibration energy harvesting. *In Recent Advances in Renewable Energy Systems*, 61–68. https://doi.org/10.1007/978-981-19-1581-9_7

Subekti, S., Guntur, H. L., Syaifudin, A., & Hendrowati, W. (2025). The influence of electromagnetic position on the elastically supported cylinder due to the influence of wind speed as an alternative energy. In *AIP Conference Proceedings* (Vol. 3320, No. 1, p. 050004). AIP Publishing LLC.

Suryadi, A., Subekti, S., & Indah, N. (2024). Investigation of harvesting energy vibrations due to the feed process on milling machines. *JTTM: Jurnal Terapan Teknik Mesin*, *5*(1), 83-89.

Syahputra, M. N. A. F., Subekti, S., & Indah, N. (2024). Effect of eccentric mass on rotor dynamics as a source of harvesting energy vibration. *JTTM: Jurnal Terapan Teknik Mesin*, *5*(1), 54-61.

Tang, B., Wang, J., Yu, X., Yang, H., Bai, R., & Tan, W. (2026). Energy harvesting of cylindrical FIV under multi-prism wake. *Renewable Energy*, *256*, 123918.

Wang, Z., Chen, J., & Yang, Y. (2022). Flow-induced vibration energy harvesting: A review of transduction mechanisms and system performance. *Renewable and Sustainable Energy Reviews*, *158*(112130). https://doi.org/10.1016/j.rser.2022.112130

Weinstein, L. A., Cacan, M. R., So, P. M., & Wright, P. K. (2012). Vortex shedding induced energy harvesting from piezoelectric materials in heating, ventilation, and air conditioning flows. *Smart Materials and Structures*, *21*(4), 045003.

Wu, Y., Pang, Y., Liu, L., Ye, T., Wang, L., Zhang, Z., ... & Wang, N. (2026). Design and Optimization of an Electromagnetic Vibration Energy Harvester. *Journal of Vibration Engineering & Technologies*, *14*(2), 54.

Zhang, Y., Liu, Z., Wang, X., & Li, H. (2024). Recent advances in flow-induced vibration energy harvesting: Mechanisms, optimization, and applications. *Energy Conversion and Management*, *297*, 117793. https://doi.org/10.1016/j.enconman.2023.117793

Zhao, L., Tang, L., & Yang, Y. (2021). Enhanced performance of vortex-induced vibration energy harvesting by wake interference. *Journal of Fluids and Structures*, *103*, 103266. https://doi.org/10.1016/j.jfluidstructs.2021.103266

Zhu, G., Li, S., & Yang, Y. (2023). Broadband vortex-induced vibration energy harvesting using nonlinear stiffness. *Mechanical Systems and Signal Processing*, *298*, 117189. https://doi.org/0.1016/j.apenergy.2021.117189